Measurement of the 4He(6He,6He)4He cross section with a 4He-implanted Al target

Raabe, R.; Weissman, L.; Andreyev, A.; Angulo, C.; Baye, D.; Bradfield Smith, W.; Cherubini, S.; Davinson, T.; Descouvemont, P.; Di Pietro, A.; Huyse, M.; Laird, A. M.; Mueller, W. F.; Musumarra, A.; Ostrowski, A.; Piechaczek, A.; Shotter, A.; Terwagne, Guy; Van Duppen, P.; Wöhr, A.

Published in:
Nuclear physics A

Publication date:
2002

Document Version
Peer reviewed version

ELSEVIER

Nuclear Physics A 701 (2002) 387c–393c

NUCLEAR PHYSICS A

www.elsevier.com/locate/npe

Measurement of the ^{4}He(^{6}He, ^{6}He)^{4}He cross section with a ^{4}He-implanted Al target

R. Raabe [b,*], L. Weissman [b,1], A. Andreyev [b,2], C. Angulo [a], D. Baye [c], W. Bradfield-Smith [d], S. Cherubini [a], T. Davinson [d], P. Descouvemont [c], A. Di Pietro [d,3], M. Huyse [b], A.M. Laird [d], W.F. Mueller [b], A. Musumarra [a,3], A. Ostrowski [d], A. Piechaczek [b,4], A. Shotter [d], G. Terwagne [e], P. Van Duppen [b], A. Wöhr [b,5]

[a] *Institut de Physique Nucléaire, Université Catholique de Louvain, B-1348 Louvain-la-Neuve, Belgium*
[b] *Instituut voor Kern- en Stralingsfysica, University of Leuven, B-3001 Leuven, Belgium*
[c] *Physique Nucléaire Théorique et Physique Mathématique, CP 229, Université Libre de Bruxelles, B-1050 Brussels, Belgium*
[d] *Department of Physics & Astronomy, University of Edinburgh, Edinburgh EH9 3JZ, United Kingdom*
[e] *Laboratoire Interfacultaire d'Analyses par Réactions Nucléaires, Facultes Universitaires Notre-Dame de la Paix, B-5000 Namur, Belgium*

Abstract

In order to obtain information on a possible two-neutron component in the ^{6}He wavefunction, we investigated the ^{4}He(^{6}He, ^{6}He)^{4}He elastic scattering at beam energies of 29.1, 29.6 and 40 MeV and at center-of-mass angles between 20 and 163 degrees. The experiments were performed at the ARENAS[3] Radioactive Ion Beam Facility in Louvain-La-Neuve. We used a ^{4}He-implanted aluminium foil as a target. A ^{4}He thickness of about 2–3 $\times$ 10^{17} particles/cm^2 was obtained implanting ^{4}He nuclei at energies between 20 and 80 keV in 0.7-μm-thick foils. Data collected in a larger angular range than previous measurements give additional evidence for the 2n-transfer process to take place in the ^{4}He(^{6}He, ^{6}He)^{4}He scattering. Our results demonstrate the possibility of

* Corresponding author.
E-mail address: riccardo.raabe@fys.kuleuven.ac.be (R. Raabe).

[1] Present address: ISOLDE, CERN, EP Division, CH-1211 Geneva 23, Switzerland.

[2] Permanent address: FLNP, Joint Institute for Nuclear Research, 141980 Dubna, Moscow region, Russia.

[3] Present address: Istituto Nazionale di Fisica Nucleare, Laboratori Nazionali del Sud, I-95123 Catania, Italy.

[4] Present address: Department of Physics and Astronomy, Louisiana State University, Baton Rouge, LA 70803, USA.

[5] Present address: Department of Physics, University of Oxford, Oxford OX1 3PU, United Kingdom.

0375-9474/02/$ – see front matter
PII: S0375-9474(01)01616-5

using a ^{4}He-implanted target in experiments with low-intensity beams, like radioactive beams, where deterioration of the target is irrelevant.

Keywords: Halo nuclei; Implanted target

Halo nuclei have so far initiated a large number of experimental and theoretical investigations [1,2]. While ^{11}Li is the showcase of a halo nucleus, ^{6}He is at this moment a much better candidate for understanding the experimental results by detailed three-body calculations (^{4}He, n, n). This is due to the fact that the ^{4}He–n and n–n interactions are well-known, while the ^{9}Li–n interaction is not. This three-body approach allows also the prediction of properties of the 2n-component in ^{6}He; however, experimental data that can reveal information on this aspect is rare.

We performed an experiment at the ARENAS^3 [3] Radioactive Ion Beam Facility in Louvain-La-Neuve, Belgium, to search for the elastic transfer of the 2n-cluster in the elastic scattering of ^{6}He on a ^{4}He target in inverse kinematics. The energy range of the ^{6}He radioactive beam in Louvain-la-Neuve enlarges the domain available for investigations of elastic-scattering and fusion processes (studied at higher energies in Dubna [4,5]), allowing measurements around the Coulomb barrier. Very accurate results can be achieved exploiting the high intensity and purity of the beam.

Measurements were carried out at beam energies of 29.1, 29.6 and 40 MeV, corresponding to center-of-mass energies on the ^{4}He target of 11.6 and 15.9 MeV. Assuming the cluster structure of ^{6}He, elastic two-neutron transfer is expected to occur between the two α cores [6]. Its observation and interpretation should provide information on the spatial and momentum correlation of the two valence neutrons in ^{6}He.

In our first measurements we used a gas cell of 1 cm thickness, containing ^{4}He at 500 mbar pressure between an entrance Al window and an exit Kapton or Al window. Reaction products were registered using a segmented silicon detector system [7]. Details about the experimental method, results obtained and their interpretation can be found elsewhere [8]. We focus here on the development of a ^{4}He-implanted aluminium target and the results obtained using it in a new measurement of the ^{4}He(^{6}He, ^{6}He)^{4}He cross section.

The use of a gas target ensured a large ^{4}He thickness (1.2×10^{19} atoms/cm^2), providing good statistics for the events of interest. However, it had some disadvantages; the main ones are: the large size of the cell, which introduced uncertainties in the kinematic reconstruction of the scattering events; the relatively thick (1.8 mg/cm^2 Kapton or 2.3 mg/cm^2 Al) exit window, which stopped particles scattered with low energies, preventing the detection of scattering events at small and large center-of-mass angles. Due to the latter, data points obtained with the gas target were limited to the range from 50 to 140 degrees in the center-of-mass. Therefore, the development of a ^{4}He-implanted Al target was undertaken in order to measure cross-section data in a larger angular range.

The use of ion-implanted targets is not a novel idea. An important limiting factor for the application of this method is probably the deterioration of the targets due to beam bombardment [9] (such limitations are not important for experiments not dedicated to cross-section measurements [10,11]). However, intensities of radioactive beams are orders

of magnitude lower compared to stable beams, even in the best cases. This makes the problem of target deterioration irrelevant.

Details about the development of the implanted targets can be found in [12]. They were prepared at the Leuven off-line isotope separator by using ^{4}He beams of various energies. We chose thin Al foils as implantation host, since we needed to minimize the energy losses of the scattered ^{4}He and ^{6}He particles in the host material itself. The Al-foil thickness was measured by weighting the samples, and was found to be 0.68 ± 0.02 μm. Several probe targets were prepared, and the details on the fluences and beam energies are listed in Table 1. During implantation the foils were mounted on an Al plate to provide heat transfer. Unfortunately due to the small thickness and fragility of the host foils it was very difficult to provide a reliable thermal contact with the backing plate. Therefore, in order to keep the target heating low, the He^+ current density was kept below 4 μA/cm^2.

To check the retained He content we have performed proton RBS measurements using the new Tandetron accelerator at the LARN laboratory of the University of Namur [13]. The RBS measurements were carried out using a 2.2 MeV proton beam. The energy was chosen to enhance the ^{4}He(p, p)^{4}He cross-section σ_{He} exploiting the strong resonance at 2.5 MeV proton energy, corresponding to the ground state of ^{5}Li. The ^{27}Al(p, p)^{27}Al cross section is equal to the corresponding Rutherford value at this particular proton energy. The ratio of σ_{He} to the Rutherford cross section at 160 degrees of proton scattering angle, where two Si detectors were placed, amounts to a factor of 250 [14]. In Fig. 1 the RBS spectrum from a nonimplanted sample (a) is compared with the one from target #3 (b). In both spectra, beside the strong RBS Al peak, two resolved peaks of ^{16}O and two resolved peaks of ^{12}C corresponding to the aluminium oxide and carbon layers at the front and the rear foil surfaces are clearly visible. In the low-energy region the background is very small, which allowed an accurate measurement of the He content. A weak, well-separated peak

Table 1
^{4}He fluences in the Al foils. For samples #3, #8, #9 and #10 (#9 was used in the ^{6}He–^{4}He experiment) implantation was performed on both sides

Foil	At 20 keV	At 30 keV	At 50 keV	At 80 keV	Total
# 1	1.0×10^{17}		0	0	1.0×10^{17}
# 2	0		0	1.0×10^{17}	1.0×10^{17}
# 3	$2 \times 1.2 \times 10^{17}$		$2 \times 1.0 \times 10^{17}$	$2 \times 0.3 \times 10^{17}$	5.0×10^{17}
# 4				1.0×10^{18}	1.0×10^{18}
# 5			1.0×10^{18}		1.0×10^{18}
# 6			2.0×10^{18}		2.0×10^{18}
# 7			1.0×10^{18}		1.0×10^{18}
# 8		$2 \times 2.0 \times 10^{17}$			4.0×10^{17}
# 9		$2 \times 4.0 \times 10^{17}$			8.0×10^{17}
# 10		$2 \times 1.1 \times 10^{17}$			7.1×10^{17}
# 11		3.0×10^{18}			3.0×10^{18}

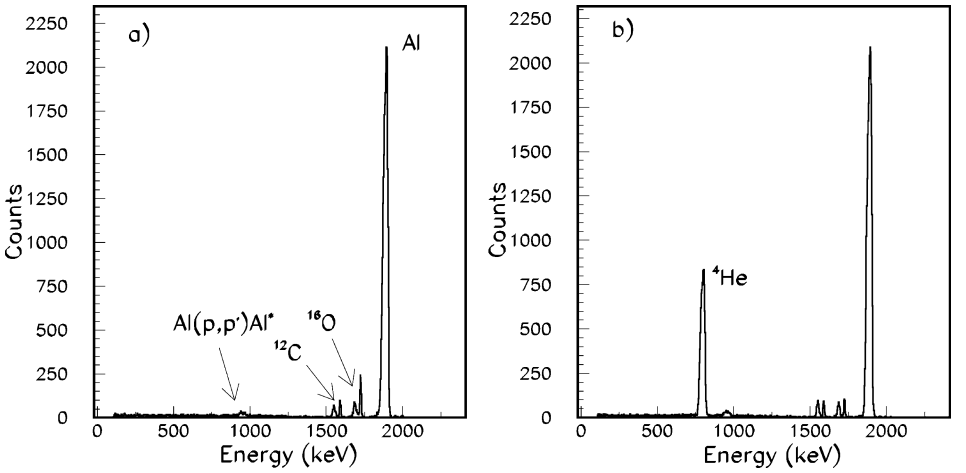

Fig. 1. The RBS spectra of (a) the nonimplanted Al sample and (b) target #3. See text for details.

Table 2
Results of the RBS measurements: measured ^{4}He thickness in the different foils

Foil	^{4}He content (at/cm^2)	^{4}He at. %	Retention (%)
# 1	$(4.98 \pm 0.18) \times 10^{16}$	1.2	50
# 2	$(3.02 \pm 0.14) \times 10^{16}$	0.7	30
# 3	$(2.20 \pm 0.07) \times 10^{17}$	5.4	44
# 4	$(5.51 \pm 0.03) \times 10^{16}$	1.3	6
# 5	$(1.12 \pm 0.06) \times 10^{17}$	2.7	11
# 6	$(1.11 \pm 0.06) \times 10^{17}$	2.7	6
# 7	$(1.43 \pm 0.07) \times 10^{17}$	3.5	15
# 8	$(1.32 \pm 0.07) \times 10^{17}$	3.2	33
# 9	$(2.72 \pm 0.14) \times 10^{17}$	6.6	34
# 10	$(2.16 \pm 0.11) \times 10^{17}$	5.3	31
# 11	$(1.61 \pm 0.14) \times 10^{17}$	2.7	5

around 900 keV corresponding to a nonelastic ^{27}Al(p, p′)^{27}Al* scattering is also observed. The strong ^{4}He peak is observed in the implanted foil, see Fig. 1b.

The He content was determined from the ratios of the integrals of the He and Al RBS peaks, knowing the values of the ^{4}He(p, p)^{4}He and ^{27}Al(p, p)^{27}Al scattering cross sections and the thickness of the Al foils. The main error comes from the uncertainty on the foil thickness (3%). The results are shown in Table 2 and Fig. 2: here the retention (ratio between the number of atoms staying in the foil and the total number of implanted atoms) is shown as function of the implanted dose. The points in Fig. 2 are rather scattered, because implantations were carried out in different conditions (implantation

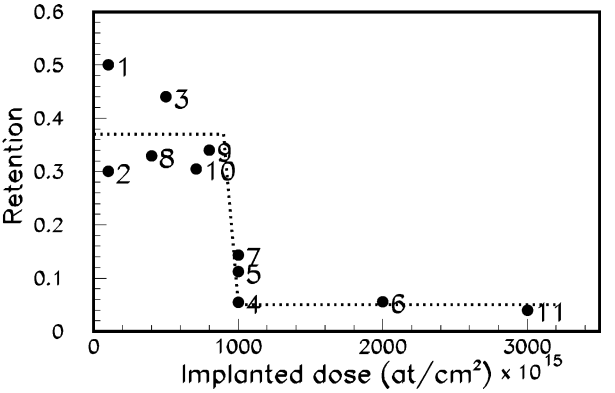

Fig. 2. ^{4}He retention in the different targets, plotted as function of the fluence. The numbers next to the data points identify the target according to Table 1 and 2. The dotted line is only to guide the eye.

energy, ^{4}He current, thermal contact) and some foils were in fact to some extent damaged. Nevertheless, a trend is visible: the retention looks constant up to a critical fluence, dropping dramatically beyond this limit. This appears to be around 7–8 $\times$ 10^{17} at/cm^2 ($\simeq$ 7% atomic concentration for a 0.7 μm Al foil), confirming previous studies [15–17]. To pin down the influence of the target heating factor on the He retention value we have implanted a higher dose, 3 $\times$ 10^{18} at/cm^2, into a 0.7 mg/cm^2 Al foil evaporated on a thick copper substrate. The latter has been consequently dissolved in a 7N HNO_3 solution. Such technique provided a good thermal contact during implantation avoiding target heating [18]. The RBS analysis of this target, #11 in Tables 1 and 2, yielded a low He content. Therefore, it seems that even with a good heat transfer the He retention drops drastically for a high fluence. The content levels of ^{4}He in the different targets were measured again after some weeks time, and found to be the same: the long time elapsed did not cause a serious diffusion out of the host foil, even though no particular procedure was followed to store the foils.

We used target #9 for the ^{4}He(^{6}He, ^{6}He)^{4}He cross-section measurement at Louvain-la-Neuve. The ^{4}He thickness was 2.7 $\times$ 10^{17} cm^{-2}, almost a factor 50 less than the thickness of the gas target previously used. However, the increased ^{6}He radioactive beam intensity and irradiation time allowed to perform the measurement successfully. The ^{6}He beam (29.1 MeV) had an average intensity of 7.7 $\times$ 10^5 pps during about 3 consecutive days. The experimental setup and subsequent analysis of the collected data were similar to the one described in [8]. The resulting cross-section data are shown in Fig. 3, where the absolute ^{4}He(^{6}He, ^{6}He)^{4}He elastic cross-section is plotted against the center-of-mass scattering angle. Filled circles correspond to data collected using the implanted target, compared to the ones collected with the gas cell (open circles). The solid curve was obtained in the analysis of the previous data sets [8] using the double-folding potential described in [19], including a parity-dependent term which takes into account the two-neutron transfer process. The curve reproduces well the new data points; if a fit of the potential parameters is performed, no appreciable changes are obtained (dotted curve). This supports the conclusions reported in [8], that the elastic 2n-transfer process is present in the

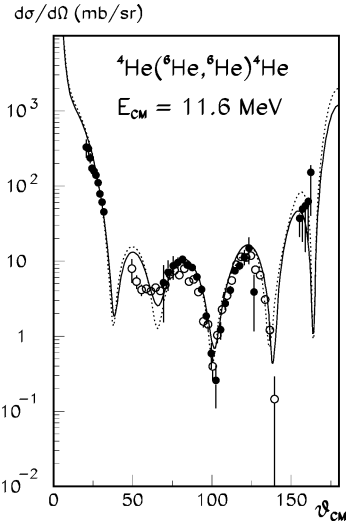

Fig. 3. Measured ^{4}He(^{6}He, ^{6}He)^{4}He differential cross section. The full curve was obtained fitting the previous sets of data [8] using a double folding potential [19] including a parity-dependent term. The dotted curve was obtained fitting the same potential to the new data points.

^{4}He(^{6}He, ^{6}He)^{4}He scattering at 11.6 MeV center-of-mass energy. The large cross section measured between 155 and 163 degrees in the center-of-mass is an additional evidence for the transfer process taking place in the reaction. These data points cannot be reproduced by a fit using a potential (either the double-folding or an optical model) that does not include the parity-dependent term. Further investigation is planned using other reaction models. Among others, special attention is dedicated to the parameter-free $\alpha + {}^6$He scattering potential calculated in the framework of the resonating group method [20,21].

In conclusion, we have used a ^{4}He-implanted Al target to measure the ^{4}He(^{6}He, ^{6}He)^{4}He cross section at a beam energy of 29.6 MeV. The thin Al foil allowed low-energy, large-angle scattered particles to escape from the target. The angular range covered using this target includes data points from 20 to 163 degrees in the center of mass, adding new information with respect to our previous measurements. Our results demonstrate the possibility of using a ^{4}He-implanted target in experiments with low-intensity beams, like radioactive beams, where deterioration of the target is irrelevant. An example is the measurement of (α, γ) and (α, p) reaction cross sections on radioactive nuclei, which is relevant to nuclear astrophysics. The use of an implanted target can be especially important for laboratories where the separation of the recoiling reaction products is possible.

References

[1] P.G. Hansen, A.S. Jensen, B. Jonson, Annu. Rev. Nucl. Part. Sci. 45 (1995) 591.
[2] I. Tanihata, J. Phys. G 22 (1996) 157.
[3] M. Gaelens, M. Huyse, P. Van Duppen, M. Loiselet, G. Ryckewaert, Nucl. Instrum. Methods B 126 (1997) 125.

[4] G.M. Ter-Akopian et al., Phys. Lett. B 426 (1998) 251.
[5] R. Wolski et al., JINR Report No. E-15-98-284, 1998.
[6] W. von Oertzen, Nucl. Phys. A 148 (1970) 529.
[7] P.J. Sellin et al., Nucl. Instrum. Methods A 311 (1992) 217.
[8] R. Raabe et al., Phys. Lett. B 458 (1999) 1.
[9] T.K. Alexander, G.C. Ball, W.N. Lennard, H. Geissel, Nucl. Phys. A 427 (1984) 526.
[10] K.H. Speidel et al., Nucl. Phys. A 552 (1993) 140.
[11] U. Grabowy et al., Nucl. Instrum. Methods B 101 (1995) 422.
[12] L. Weissman et al., Nucl. Instr. Meth. A, submitted.
[13] G. Demortier, Nucl. Instrum. Methods B 66 (1992) 51.
[14] J.R. Tesmer, M. Nastasi (Eds.), Handbook of Modern Ion Beam Material Analysis, Material Research Society, Pittsburgh, USA, 1995.
[15] S.E. Donnelly, F. Bodart, K.M. Barfoot, R. Wernz, R.P. Webb, Thin Solid Films 94 (1982) 289.
[16] W. Jäger, R. Manzke, H. Trinkaus, G. Crecelius, R. Zeller, J. Fink, H.L. Bay, J. Nucl. Mater. 111–112 (1982) 674.
[17] K.L. Wilson, G.J. Thomas, J. Nucl. Mater. 63 (1976) 266.
[18] G. Terwagne, S. Lucas, F. Bodart, G. Sorensen, H. Jensen, Nucl. Instrum. Methods B 45 (1990) 95.
[19] D. Baye, L. Desorgher, D. Guillain, D. Herschkowitz, Phys. Rev. C 54 (1996) 2563.
[20] D. Baye, P. Descouvemont, Y. Suzuki, K. Varga, Phys. Rev. C 59 (1999) 817.
[21] P. Descouvemont, private communication.